***Graphical Abstract**

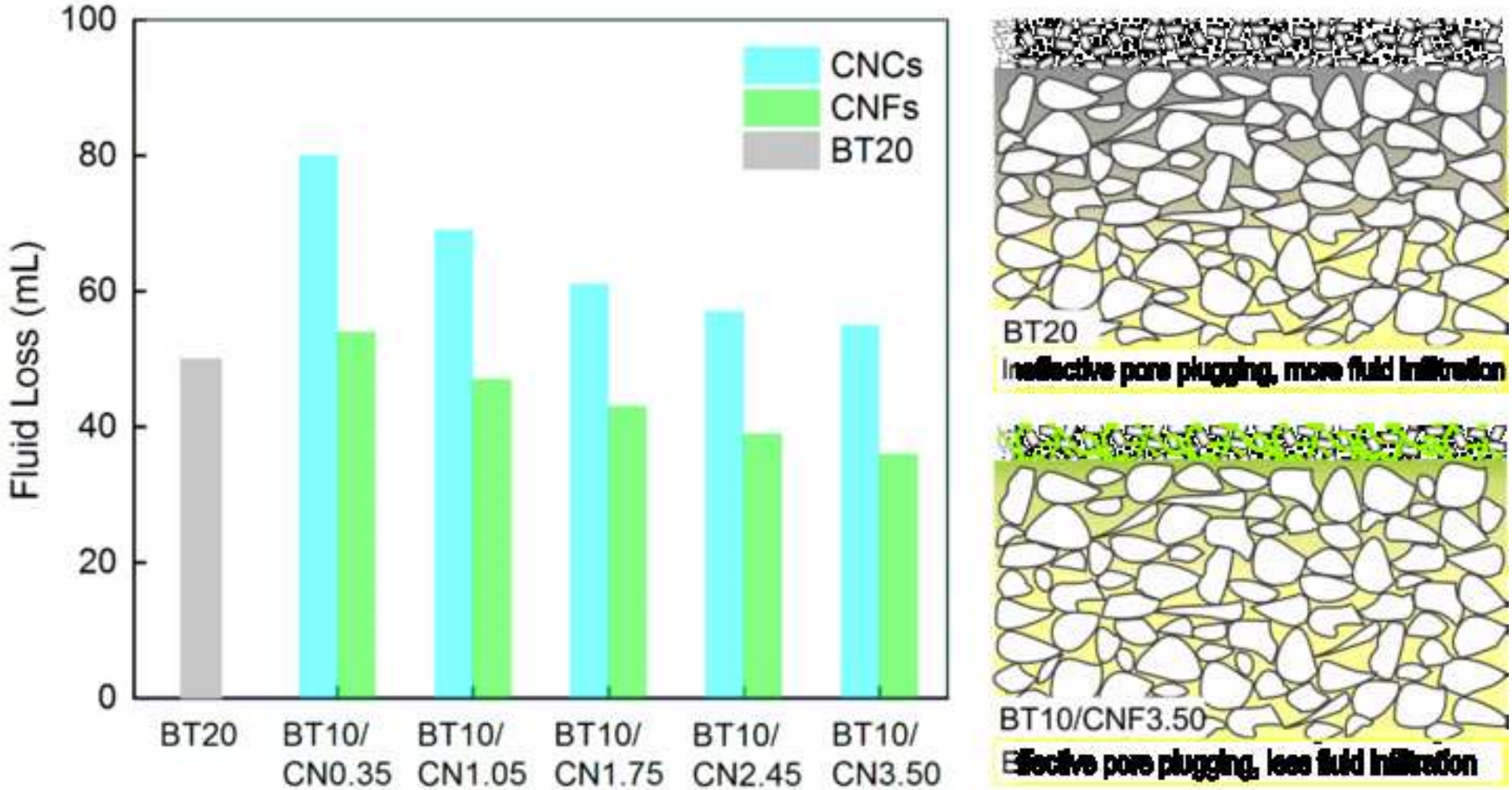

Water-Based Bentonite Drilling Fluids Modified by Novel Biopolymer for Minimizing Fluid Loss and Formation Damage

Kunlin Song [a], *Qinglin Wu* [a*], *Meichun Li* [a], *Suxia Ren* [b], *Lili Dong* [b], *Xiuqiang Zhang* [b], *Tingzhou Lei* [b*], *and Yoichi Kojima* [c]

[a] School of Renewable Natural Resources, Louisiana State University, Baton Rouge, LA 70803, USA

[b] Key Biomass Energy Laboratory of Henan Province, Zhengzhou, 450008, Henan, China

[c] Department of Environment & Forest Resources Science Faculty of Agriculture, Shizuoka University, Shizuoka 422-8529, Japan

[*] Corresponding authors: wuqing@lsu.edu (Qinglin Wu); leitingzhou@163.com (Tingzhou Lei)

Abstract

Cellulose nanoparticles (CNPs), including cellulose nanocrystals (CNCs) and cellulose nanofibers (CNFs), were used as an environmentally friendly and high performance additive in water-based bentonite drilling fluids for minimizing fluid loss and formation damage. The effects of CNP dimension and concentration on the rheological and filtration properties of the fluids were investigated. With half of the bentonite in the fluid replaced by a small fraction of CNPs, the resultant fluids showed excellent shear thinning behavior and the fluids' viscosity, yield point, and gel strength increased with the concentrations of CNPs. The addition of CNPs did not produce a pronounced effect in loss of the fluids under low temperature and low pressure (LTLP) conditions. However, reduced fluid loss and formation damage were observed with use of CNPs at a higher temperature and pressure condition, demonstrating CNP's potentials for high temperature and high pressure well applications. Additionally, CNCs and CNFs functioned differently in the rheological and filtration properties of the fluids, attributed to their distinct morphology and surface functionality, which could be controlled to maximize the performance of the fluids.

Keywords: Water-based drilling fluids; Nanocellulose; Rheology; Fluid filtration; Formation damage

25 **Graphical Abstract**

26

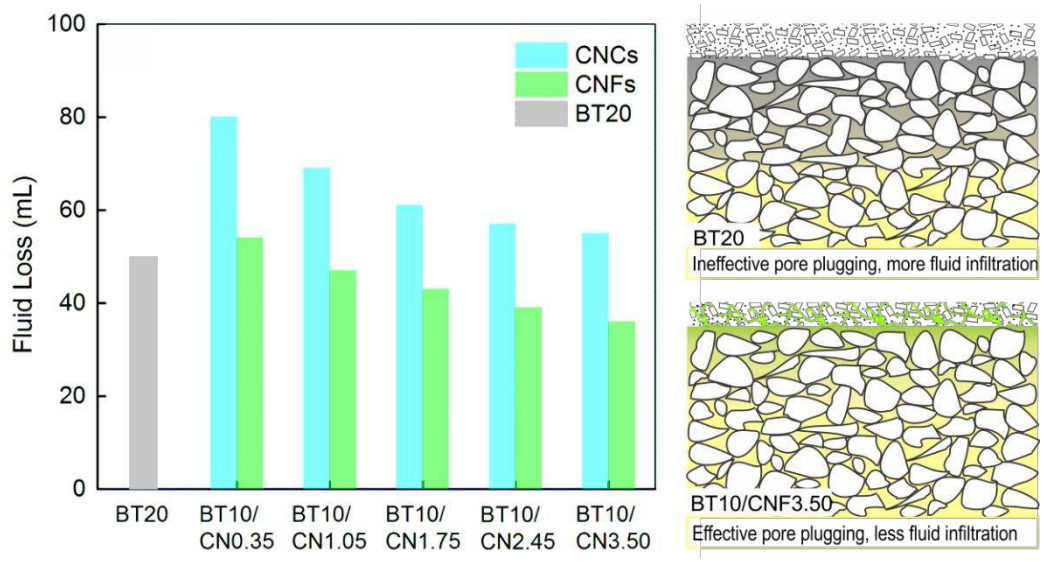

27

1. Introduction

Drilling fluids perform essential tasks including controlling formation pressures, minimizing formation damage, maintaining wellbore stability, suspending and carrying out cuttings, and cooling as well as lubricating drilling bits [1-3]. Successful drilling operations are highly dependent on the selection of the fluids with desirable properties, which are determined by their rheological and fluid filtration properties to a large extent. Lack in required performance of the fluids may cause severe drilling problems such as differential sticking, lost circulation, wellbore instability, and formation damage. These problems become more serious in deep drilling due to deteriorations of fluid properties resulted from a considerable increase in temperature and pressure [4]. Bentonite (BT) is commonly used in drilling fluids due to its excellent colloidal properties. However, a high concentration of BT in fluids can lower drilling efficiency and even result in problems such as differential sticking, inefficient wellbore cleaning, and formation damage. Additionally, the flocculation of BT at a higher temperature and pressure condition is one of main factors leading to the malfunctions of drilling fluids [5]. Therefore, it is highly desirable to find various additives to compensate for BT deficiencies.

Recently, nanotechnology has provided opportunities to the development of a new generation of fluids defined as smart fluids, in which nanoparticles are added for improved and enhanced drilling and oil recovery [4, 6-8]. Due to the unique characteristics including small dimension and high surface area to volume ratio of nanoparticles, they have attracted an increasing attention as additives in fluids by enhancing drilling performance, including eliminating differential pipe sticking, maintaining borehole stability, reducing fluid loss, improving cutting removal ability, reducing formation damage, and enhancing oil and gas recovery [9]. In order to obtain these performance improvements, various nano additives in drilling fluids were studied. Graphene oxide presented well performance as a filtration additive in water-based fluids at a very low concentration (0.2 wt%), giving an average API fluid loss of 6.1 mL and a filter cake of 20 μm thick compared to a fluid loss of 7.2 mL and a filter cake of 290 μm thick from a standard fluid in the oil industry [10]. Carbon nanotubes were dispersed in drilling fluids to enhance thermal conductivity and filtration properties [11]. A core-shell structured nano silica composite was prepared and added into drilling

fluids, which showed improved rheology, filtration, lubricity, and pore plugging ability [12]. In addition, a variety of nano metallic oxide such as CuO, ZnO, and TiO_2 was also investigated as functional additives to improve performance of drilling fluids, especially at high temperature and high pressure conditions [13-15]. Although these nanoparticles in the fluids presented superior properties, most of them were expensive to prepare, nonrenewable, and nonbiodegradable. With more stringent control of pollution, safe risk, and cost, it is crucial to apply more environmentally friendly and cost-effective nanoparticle as additives in drilling fluids.

Nanocellulose as an earth abundant, biodegradable, and renewable biopolymer nanomaterial receives great attention, due to its excellent characteristics such as nanoscale dimensions, a high surface area to volume ratio, high mechanical strength/weight performance, large flexibility, and desirable colloidal properties [16-19]. Cellulose nanoparticles (CNPs) can be extracted from various cellulosic resources like wood, cotton, and chitin by mechanical treatment, acid hydrolysis, enzymatic hydrolysis, or a combination of these methods. Based on the morphology of CNPs, it can be categorized as cellulose nanocrystals (CNCs) and cellulose nanofibers (CNFs). CNCs have a rod-like shape with several nanometers in width and 50-500 nm in length, while CNFs exhibit highly entangled network and a larger aspect ratio with 4-20 nm in width and several micrometers in length [20]. The differences in the size and shape between CNCs and CNFs can result in diverse interface effects and different performance in structure and properties of materials. The versatility of cellulose materials makes room for consideration in a wide range of revolutionary applications[21, 22]. CNPs have recently come into view of oilfield researchers and have captured their great interest, judged by the related patents applied in the past several years. CNCs were added in well fluids to increase the viscosity of water-based well service fluids, such as kill pill, fracturing fluid, and gravel packing fluid, and to improve the strength of cement [23]. CNCs from chitin were used as additives in cement and wellbore fluids to inhibit corrosion in pipelines and downhole tools [24]. Additionally, CNCs were added in a variety of well fluids such as fracturing fluids, stimulation fluids, completion fluids, conformance control fluids, and drilling fluids for treating a subterranean formation by replacing conventional polymers in these fluids [25]. The addition of CNPs can help make drilling fluids more environmentally friendly. However,

these previous patent applications only outline general principles for applying CNPs in drilling fluids. Further systematic scientific investigations on fluid formulation and control mechanism are greatly needed. Specifically, morphological effects of CNPs on rheological and filtration properties of the fluids as well as characteristics of formed filter cakes, especially at a higher temperature and pressure condition, are essential to provide an in-depth understanding of functions of CNPs in the fluids.

The objective of this study was to evaluate CNPs as a functional additive in drilling fluids to minimize fluid loss and formation damage. Novel, low-cost, and ecologically friendly water-based fluids containing CNPs, BT, and other additives including sodium hydroxide, lignite, polyanionic cellulose (PAC), and Rev dust were developed for enhancing the fluid performance. The effect of CNP morphology and concentrations on the rheological and filtration properties of the fluids was investigated. The filtration loss of the fluids at low temperature and low pressure (LTLP) and a higher temperature and pressure condition was studied. Special emphasis was placed on the filter cake formation characteristics of the fluids to demonstrate the effectiveness and performance of CNPs in reducing formation damage.

2. Materials and Methods

2.1 Materials

Sulfuric acid and sodium hydroxide (ACS reagent) were purchased from Sigma-Aldrich Corp. (St. Louis, MO, USA.). Wyoming sodium BT was provided by Baroid Industrial Drilling Products Inc. (Houston, TX, USA). Lignite and PAC (white powder of carboxymethyl cellulose with a high purity and large substitution degree of carboxylic groups (>0.90) and bulk density of 881 kg/m^3) were provided by Halliburton Company (Houston, TX, USA). Rev dust (powder of montmorillonite clay simulating drilled cutting fines) was provided by Turbo-Chem International Inc. (Dr. Scott, LA, USA). Two types of CNPs were used in this study. CNFs (Celish KY 100-S grade, 25 wt% solid content) was directly supplied by Daicel Chemical Industries, Ltd. (Tokyo, Japan). CNCs were produced by breaking down the CNFs using acid hydrolysis [26, 27]. Specifically, the CNC suspensions were produced through the hydrolysis of CNFs using 64% sulfuric acid at 45ºC for 1 h. Excess water was added to terminate the reaction and the suspensions were placed in regenerated cellulose dialysis tubes with a molecular weight cutoff of 12000-

14000 and dialyzed against water until the pH reached around 7. To increase the dispersion of the CNCs in water, a further mechanical separation by a high-pressure homogenizer (Microfluidizer M-110P, Microfluidics Corp., Newton, MA, USA) were applied to produce stable water suspensions of CNCs with an average concentration of 1.5 wt%. The surface morphologies of CNCs and CNFs were observed under a transmission electron microscope (TEM, JEOL 100 CX, Peabody, MA, USA).

2.2 Formulations of drilling fluids

Table 1 Formulations of the water-based bentonite drilling fluids in this study

Formulations [a]	BT (g)	CN (g) [b]	NaOH (g)	Lignite (g)	PAC (g)	Rev Dust (g)
BT20	20	0	0.25	1	0.5	5
BT10	10	0	0.25	1	0.5	5
BT10/CN0.35	10	0.35	0.25	1	0.5	5
BT10/CN1.05	10	1.05	0.25	1	0.5	5
BT10/CN1.75	10	1.75	0.25	1	0.5	5
BT10/CN2.45	10	2.45	0.25	1	0.5	5
BT10/CN3.50	10	3.50	0.25	1	0.5	5

[a] All the formulations were prepared in 350 mL distilled water; [b] CN denotes CNCs or CNFs

Water-based drilling fluids consisting of BT (main component of drilling fluids for viscosity and filtration control), CNPs, and other additives including sodium hydroxide, lignite, PAC, and Rev dust were prepared following commercial water-based fluid formulations currently used in drilling fields. The concentrations of these components are listed in Table 1. All the fluids were prepared with 350 mL distilled water in a laboratory stainless steel barrel. The BT and CNPs (i.e., CNCs and CNFs) varied from 10 g to 20 g and from 0.35 g to 3.50 g, respectively. The contents of sodium hydroxide (0.25 g), lignite (1 g), PAC (0.5 g), and Rev Dust (5 g) were kept constant for each experiment, and they were used as a pH control agent, deflocculant, filtration control agent, and substance of simulating drilling solids, respectively.

2.3 Rheological measurement

Rheological properties of the fluids were measured at room temperature (25 ˚C) and standard atmospheric pressure (0.1 MPa) using an industrial rotating viscometer (NL Baroid, NL Industries, Inc.,

Houston, TX). The apparent viscosity (μ_α), plastic viscosity (μ_p), and yield point (τ_y) were calculated using the following formulas according to American Petroleum Institute (API) recommended standard procedure for testing water-based drilling fluids.

$$\mu_\alpha = \theta_{600}/2 \quad (1)$$

$$\mu_p = \theta_{600} - \theta_{300} \quad (2)$$

$$\tau_y = \theta_{300} - \mu_p \quad (3)$$

where θ_{300} and θ_{600} were dial readings from the viscometer at a rotating speed of 300 and 600 rpm, respectively. To reach steady state conditions, the fluids were stirred for 10 mins prior to rheological measurements. In addition, the gel strength, including Gel_{in} and Gel_{10min} of the fluids, was obtained by recording the maximum dial readings at 3 rpm after the fluid was stirred at 600 rpm for 1 min followed by maintaining static for 10 s and 10 min, respectively. Each experiment was repeated at least three times to ensure the reproducibility of the results.

2.4 Fluid filtration testing

The LTLP filtration testing was conducted using a standard filter press with a regulated CO_2 pressuring system and standard Fann filter papers (Fann Instrument Co., Houston, TX, USA). The measurements were completed at the pressure of 0.69±0.03 MPa and the temperature of 25 ˚C according to the API recommended standard procedure for testing water-based drilling fluids. The mass of the filtrate against time was measured using a digital balance, and then the volume of filtrate was calculated by its mass and density. The API fluid loss versus time was thus determined. After the measurements, the filter cakes were taken out from the cells and their thickness was recorded. Subsequently, these filter cakes were freeze-dried and coated with a thin layer of gold for observing their surface morphologies by a field emission scanning electron microscope (FE-SEM, FEI QuantaTM 3D FEG Dual Beam SEM/FIB, Hillsboro, OR, USA).

The filtration testing at a higher temperature and pressure condition (93 ˚C and 6.9 MPa) was completed using a permeability plugging apparatus (PPA) and ceramic discs (Fann Instrument Co., Houston,

TX, USA). This equipment is designed to simulate field well conditions and these discs closely simulate the structure of formation, providing a more authentic representation of downhole filtration. A 300 mL sample of the fluids was loaded into the PPA cell and a ceramic disc with an average pore throat diameter of 20 μm was then inserted. The spurt loss (V_S) was recorded at the time when the pressure initially reached 6.9 MPa. The API fluid loss (V) was calculated by the following equation:

$$V = V_S + (2 \times V_{30}) \quad (4)$$

where V_{30} was the fluid loss at 30 mins. At the end of filtration testing, thickness of the filter cakes deposited on the ceramic disks was recorded. Subsequently, the filter cakes were removed and the ceramic disks were dried and coated with a thin layer of gold prior to FE-SEM observation.

3. Results and discussion

3.1 Structure of cellulose nanoparticles

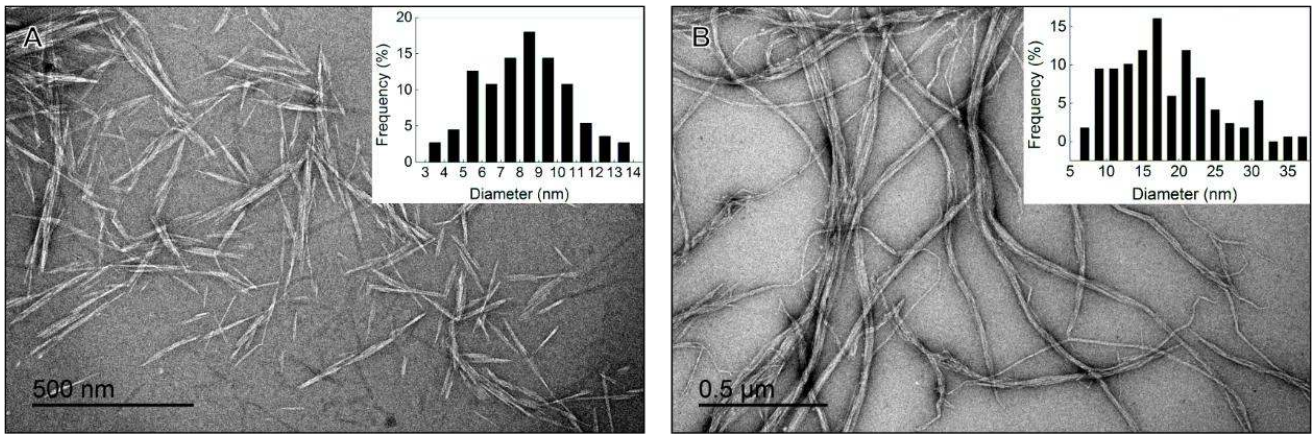

Figure 1 TEM photographs and diameter distributions (inserted plots) of the CNCs (A) and CNFs (B)

The CNCs showed needle-like or whisker shaped morphology (Figure 1A), while the CNFs exhibited highly entangled network consisting of long nanofibers (Figure 1B). The CNCs had an average width of (8.2±2.3) nm and length of (321.6±34.7) nm, giving an aspect ratio of 39±15. The average diameter of CNFs was measured to be (18.6±6.9) nm and the length was much larger in micrometers, compared to that of CNCs. Accordingly, the CNFs had a wider distribution of diameters and higher aspect ratio than these of CNCs, resulting from the aggregations and large length of CNFs. In addition, the sulfuric acid hydrolysis introduced negatively charged sulfate groups onto the surface of CNCs, as confirmed by the zeta potential

and X-ray photoelectron spectroscopy analysis in our previous work [26]. These sulfate groups resulted in more stabilized suspensions with well dispersed individual CNCs, in comparison with the CNFs without charged surfaces [28]. Due to these structural differences in dimension, shape, and surface characteristics between the CNCs and CNFs, it was expected that CNCs and CNFs produce different effects on rheological and fluid filtration properties of the fluids (elaborated in the following sections).

3.2 Rheological properties

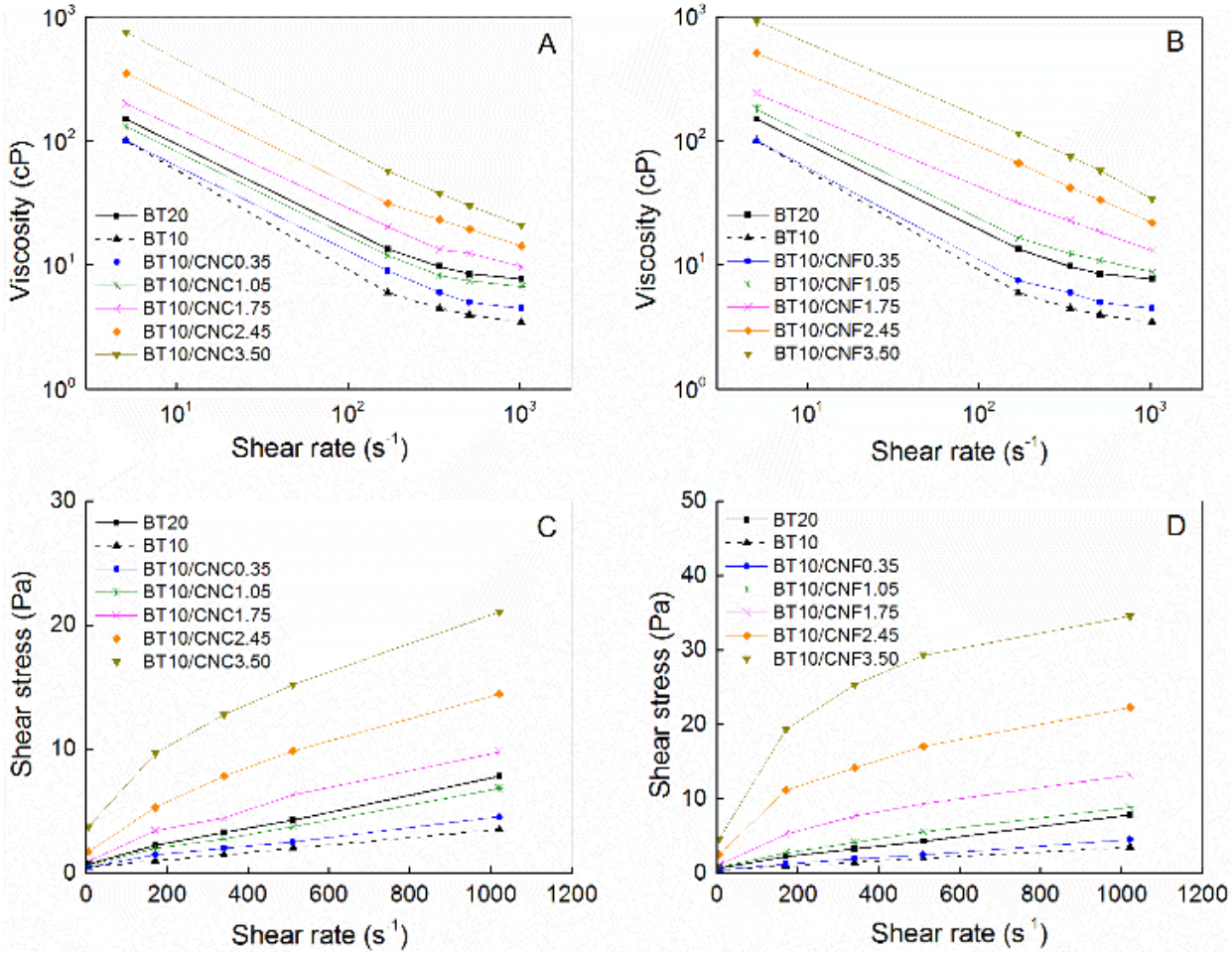

Figure 2 Viscosity and shear stress as functions of shear rates for the fluids with different concentrations of cellulose nanoparticles

Drilling fluids are commonly considered as non-Newtonian fluids with viscosity decreasing with increased shear rates [1]. High viscosity of the fluids at low rates is required to suspend drilled cuttings and carry them out of the wellbore. Low viscosity of drilling fluids at high shear rates makes the fluids to flow

182 into downhole with less resistance. Consequently, various additives were used to improve the rheological
183 performance of drilling fluids [4, 29, 30]. The CNPs was added in the fluids due to its excellent rheological
184 property, besides its abundance and environmental benefits [31]. It was found that the water suspensions of
185 CNPs showed obvious shear thinning behavior, with high viscosity at low shear rates and low viscosity at
186 high shear rates [20]. This phenomenon increased as the CNP concentration was increased, showing
187 concentration dependence at low rates and reduced concentration dependence at high rates [20, 26]. The
188 effects of CNP concentration on the rheological properties of the fluids are shown in Figure 2 and Table 2.
189 The control fluid without CNPs exhibited significant shear thinning behavior, and its calculated values of
190 apparent viscosity and plastic viscosity were 7.8 cP and 7.2 cP, respectively. When the BT content was
191 reduced by half (i.e., from 20 g to 10 g), the apparent viscosity and plastic viscosity of the fluids largely
192 decreased with the values of 3.4 cP and 2.9 cP, respectively (Table 2). Maintaining the reduced content of
193 bentonite at 10 g in the fluids, CNPs with loading levels varied from 0.35 g to 3.50 g were added. It was seen
194 that the fluids added with CNCs or CNFs still presented a marked shear thinning behavior similar to the
195 control fluid (Figure 2A and 2B), contributed by the non-Newtonian fluid properties of CNP suspensions.
196 Meanwhile, the viscosity increased with increased concentrations of CNPs in the fluids. When the content of
197 CNPs increased to 1.05 g, the apparent viscosity and plastic viscosity of the fluids added with CNCs were
198 6.8 cP and 6.0 cP and the corresponding values for the fluids with CNFs were 9.1 cP and 7.0 cP, which more
199 or less reached the level of the control fluid. By further increasing the concentration of CNPs, the viscosity,
200 yield stress, and gel strength of the fluids continued to rise. Here, it was found that the rheological
201 performance of the fluids was maintained and even improved after decreasing the content of BT and adding
202 a small amount of CNP material. This would be extremely beneficial because of the reduced solid content in
203 the fluids, which is preferred for faster drilling rate, decreased cost in solid control and fluid maintenance,
204 reduced formation damage, and improved hydraulics [29].

205

206

Table 2 Rheological properties of the drilling fluids with different contents of cellulose nnaoparticles

Formulations	μ_α (cP)	μ_p (cP)	τ_y (Pa)	Gel Strength (Pa)	
				Gel_{in}	Gel_{10min}
BT20	7.8±0.8	7.2±0.8	0.6±0.08	0.8±0.03	1.2±0.30
BT10	3.4±0.4	2.9±0.4	0.5±0.03	0.5±0.00	0.5±0.00
BT10/CNC0.35	4.5±0.5	3.9±0.1	0.5±0.03	0.5±0.00	0.6±0.05
BT10/CNC1.05	6.8±0.2	6.0±0.2	0.8±0.04	1.2±0.25	4.5±1.56
BT10/CNC1.75	9.9±1.1	7.2±1.0	2.6±0.15	1.1±0.38	6.0±0.91
BT10/CNC2.45	14.1±1.1	8.6±0.9	5.3±0.31	1.8±0.21	7.1±1.40
BT10/CNC3.50	20.3±1.6	10.7±1.9	9.2±0.37	3.9±0.36	10.9±0.49
BT10/CNF0.35	4.4±0.6	3.9±0.6	0.5±0.03	0.5±0.00	0.7±0.09
BT10/CNF1.05	9.1±1.5	7.0±2.3	2.0±0.43	0.9±0.07	1.1±0.18
BT10/CNF1.75	13.3±1.4	7.9±0.5	5.2±0.13	1.1±0.15	1.2±0.22
BT10/CNF2.45	21.0±1.1	9.9±0.4	10.6±0.69	2.3±0.21	3.0±0.46
BT10/CNF3.50	34.8±1.5	11.5±1.1	22.3±0.89	4.3±0.75	4.9±1.14

The surface morphologies of CNPs played an essential role in the rheological behavior of the fluids. At the lowest loading level (0.35 g) of CNCs or CNFs was added, the fluids had almost the same values of apparent viscosity, plastic viscosity, yield point, and gel strength (Table 2). As the content of CNPs was increase to above 0.35 g, the rheological values (excluding Gel_{10min}) of the fluids with CNCs were lower than those of the fluids added with CNFs and the differences between them became much larger with increased concentrations of CNPs. For instance, at the CNP content of 3.50 g, the fluids with CNCs (BT10/CNC3.50) had apparent viscosity, plastic viscosity, yield point, and initial gel strength values of 20.3 cP, 10.7 cP, 9.2 Pa, and 3.9 Pa, respectively; whereas the corresponding values for the fluids with CNFs (BT10/CNF3.50) were 34.8 cP, 11.5 cP, 22.3 Pa, and 4.3 Pa, respectively. These differences were attributed to the distinct surface morphologies between CNCs and CNFs. The smaller size and good dispersion of the CNCs in water made CNCs much easier to flow in the fluids under shear stress [26]. By contrast, the long dimensions of CNFs formed a highly entangled network, where the platelets of BT resided, and this system was much difficult to flow under the same shear stress. In addition, the Gel_{in} of the fluids with CNCs was slightly lower than that

of the fluids with CNFs, but the Gel_{10min} reversed. The BT10/CNC3.50 had a Gel_{10min} value of 11.1 Pa, which was much larger than 4.6 Pa for the BT10/CNF3.50 (Table 2). This was due to the stronger surface hydrogen bonding capability of CNCs in comparison with CNFs. The surfaces of CNPs had hydroxyl groups, which could form hydrogen bonding among CNPs as well as among CNPs and other components (BT, lignite, and PAC) in the fluids. The amphoteric Al-OH and Si-OH groups from broken bonds of the octahedral Al layers and tetrahedral Si layers of BT, -COOH groups from lignite, and –OH groups from PAC could also form hydrogen bonding among them and with -OH groups of CNPs. Compared to CNFs, CNCs had a higher specific surface area because of their smaller dimensions, resulting in a larger number of hydroxyl groups available on the surfaces of CNCs to form more hydrogen bonds. Accordingly, a stronger hydrogen bonding network formed in the fluids added with CNCs, making them much harder to flow (Figure 3). However, it took some time to build an effective hydrogen bonding network in the fluids. The formed network was very weak within a very short time (10 seconds used in this study) after a high speed of shear (600 rpm or 1022 s^{-1}). At this time, the gel strength (Gel_{in}) of the fluids with CNCs was still lower than that of the fluids with CNFs. Giving a longer time (10 mins), the stronger network with a larger number of hydrogen bonds was established in the fluids with CNCs. As a result, much higher shear stress was required to initiate the flow of the fluids with CNCs. This kind of strong hydrogen bonding network was not built in the fluids with CNFs, leading to its relatively lower Gel_{10min} values, compared to those of the fluids with CNCs.

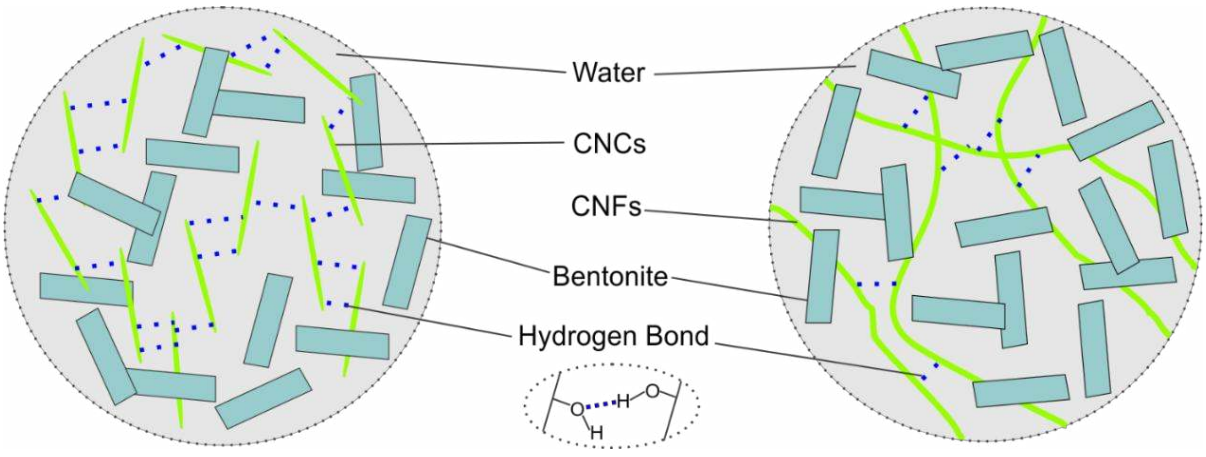

Figure 3 Schematic illustrating the formations of hydrogen bonding among CNCs and CNFs in the fluids

3.3 Fluid filtration under LTLP

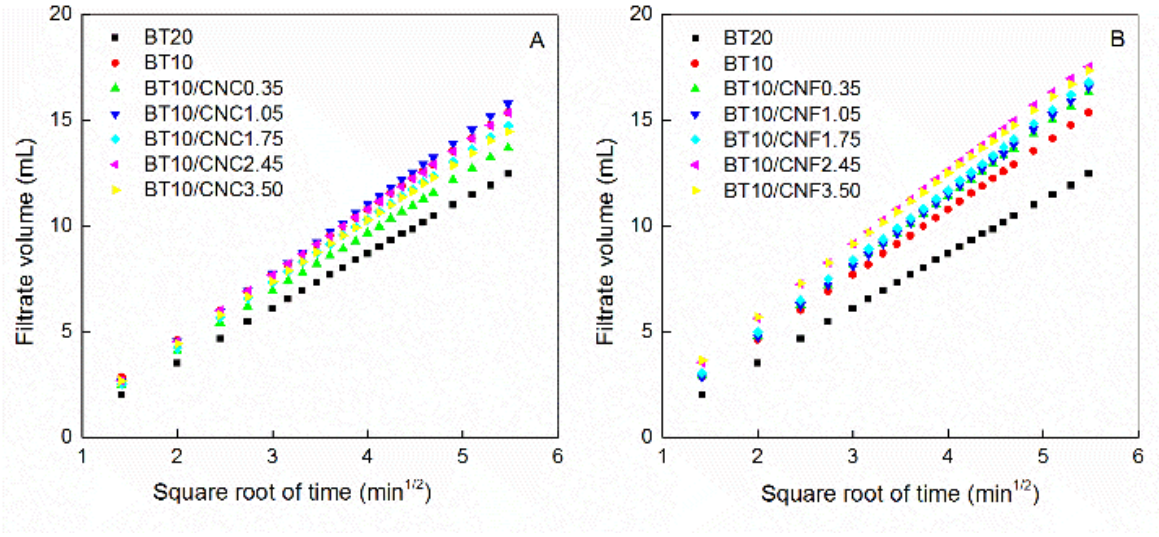

Figure 4 Filtration volume versus square root of time for the fluids under LTLP conditions

A preferred drilling fluid should have desired filtration properties such as a reasonable range of fluid loss as well as thin and dense filter cakes formed on the walls of wellbores, which could prevent lost circulation, differential sticking, and even wellbore collapse [1]. In Figure 4, the filtration volume of the fluids under LTLP conditions against the square root of time shows linear relationships. This could be explained by the Darcy's Law, which is commonly used to describe the flow of drilling fluid filtrate through the filter cakes [1, 32]. The linear relationship between filtrate volume and square root of time was expected according to the solution to Darcy's Law,

$$V_f = \sqrt{2\kappa\Delta p(\frac{f_{sc}}{f_{sm}} - 1)}A\frac{\sqrt{t}}{\sqrt{\mu}} \quad (5)$$

where V_f, t, κ, A, Δp, μ, f_{sc}, f_{sm} is filtrate volume (mL), time (s), permeability (D), cross-section area (cm^2) of filter cakes, pressure drop across filter cakes (atm), viscosity (cP) of filtrate, volume fraction of solids in the fluids, and volume fraction of solids in filter cakes. The control fluid (BT20) had a fluid loss of 12.9 mL, and the value increased to 15.4 mL when the bentonite content decreased to 10 g (Table 3). After the CNPs were added, the fluid loss was slightly larger than that of the control fluid (BT20). However, the value was not obviously different from that of BT10, with varied values in the small ranges of 13.8-15.6 mL

for the fluids with CNCs and 15.7-17.7 mL for the fluids with CNFs, respectively. This indicated that the concentration of CNPs did not have a significant effect on the filtrate volume of the drilling fluids under LTLP conditions. Additionally, it was noticed that the loss of the fluids with CNFs was a little higher than that of the fluids with CNCs, and the mechanism was attributed to the difference in the formation of filter cakes as explained in the following section.

Table 3 The API fluid loss, thickness, and permeability of filter cakes for the drilling fluids under LTLP conditions

Formulations	V_f (mL)	h_c (cm)	k (μD)	k/h_c (μD/cm)
BT20	12.9±0.4	0.13±0.02	2.31±0.13	17.4±1.8
BT10	15.4±0.5	0.10±0.02	2.22±0.21	21.7±1.2
BT10/CNC0.35	13.8±0.3	0.10±0.01	1.95±0.11	18.9±0.5
BT10/CNC1.05	15.2±0.6	0.11±0.01	2.34±0.18	21.5±3.6
BT10/CNC1.75	14.2±1.0	0.12±0.02	2.35±0.24	20.3±1.5
BT10/CNC2.45	14.5±0.9	0.17±0.02	3.39±0.29	20.4±1.2
BT10/CNC3.50	15.6±1.0	0.28±0.02	6.02±0.64	21.7±1.3
BT10/CNF0.35	15.7±0.7	0.10±0.01	2.26±0.06	21.9±1.2
BT10/CNF1.05	16.6±0.6	0.12±0.01	2.70±0.22	22.5±1.5
BT10/CNF1.75	17.1±0.4	0.16±0.01	3.67±0.17	23.0±2.0
BT10/CNF2.45	17.1±1.4	0.23±0.04	5.40±0.48	23.4±2.1
BT10/CNF3.50	17.7±0.6	0.32±0.02	7.61±0.32	23.8±0.7

The characteristics of filter cakes are shown in Table 3 and Figure 5. The thickness of filter cakes for BT20 and BT10 was 0.13 cm and 0.10 cm, respectively. When a small content (<1.75 g for CNCs and <1.05 g for CNFs) of CNPs was added into the fluids, the thickness of filter cakes almost unchanged within the values of 0.10-0.12 cm. As more CNPs were used, the thickness of filter cakes increased quickly and reached to 0.28 cm for BT10/CNC3.50 and 0.32 cm for BT10/CNF3.50. The similar trend was found for the permeability of the filter cakes calculated by the following equation,

$$\frac{dV_f}{dt} = \frac{\kappa A \Delta p}{\mu h_c} \quad (6)$$

where h_c is the thickness of filter cake (cm), respectively. To calculate the permeability, A, Δp, and μ were assumed to be constant with the values of 45 cm^2, 690 Pa, and 1×10^{-3} Pa·s, respectively. The increased thickness and permeability of filter cakes with increased loading levels of CNPs (>1.75 g for CNCs and >1.05 g for CNFs) resulted from more loose structure of cakes caused by the added CNPs, especially for CNFs (Figure 5). The CNPs and BT were not miscible and the interfaces between them could offer paths for the filtrate to flow through the filter cakes and enhanced the connectivity of pores in the filter cakes. This phenomenon became more obvious with increased concentrations of CNPs and larger dimensional fibers, resulting in relatively larger permeability of filter cakes with CNFs. Furthermore, filtrate volume was proportional to permeability but inversely proportional to thickness of filter cakes according to the above equation. Then, the ratio of permeability to cake thickness was calculated and found to fit well with the values of filtrate volume (Table 3). Consequently, the slightly higher loss of the fluids with CNFs in comparison with the fluids added by CNCs was contributed by both the increased permeability and thickness of less effective filter cakes. However, the increased permeability contributed more compared with the cake thickness.

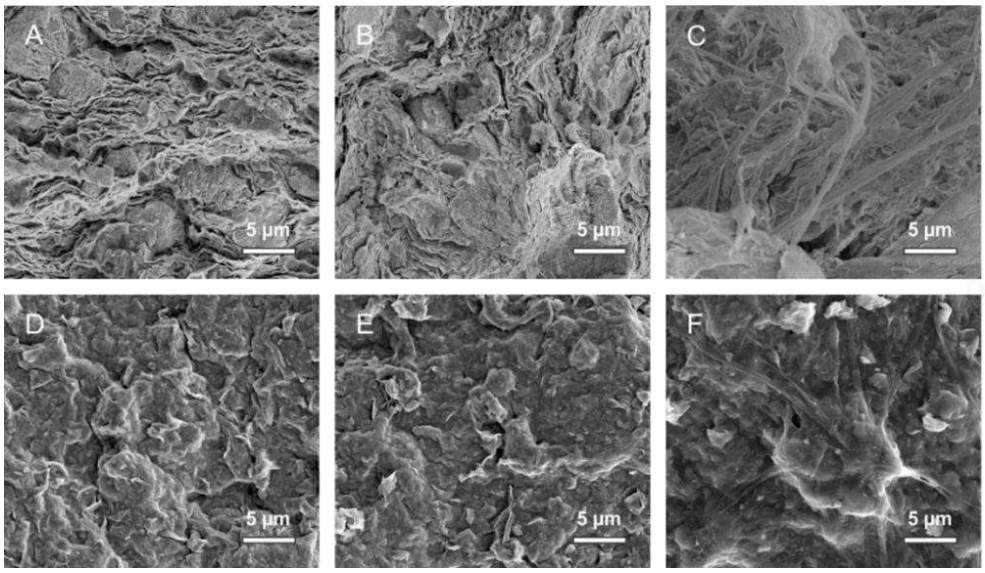

Figure 5 Cross sectional (A, B, and C) and surface (D, E, and F) FE-SEM images of the filter cakes for BT20 (A and D), BT10/CNC3.50 (B and E), and BT10/CNF3.50 (C and F) under LTLP conditions

3.4 Fluid filtration under a higher temperature and pressure condition

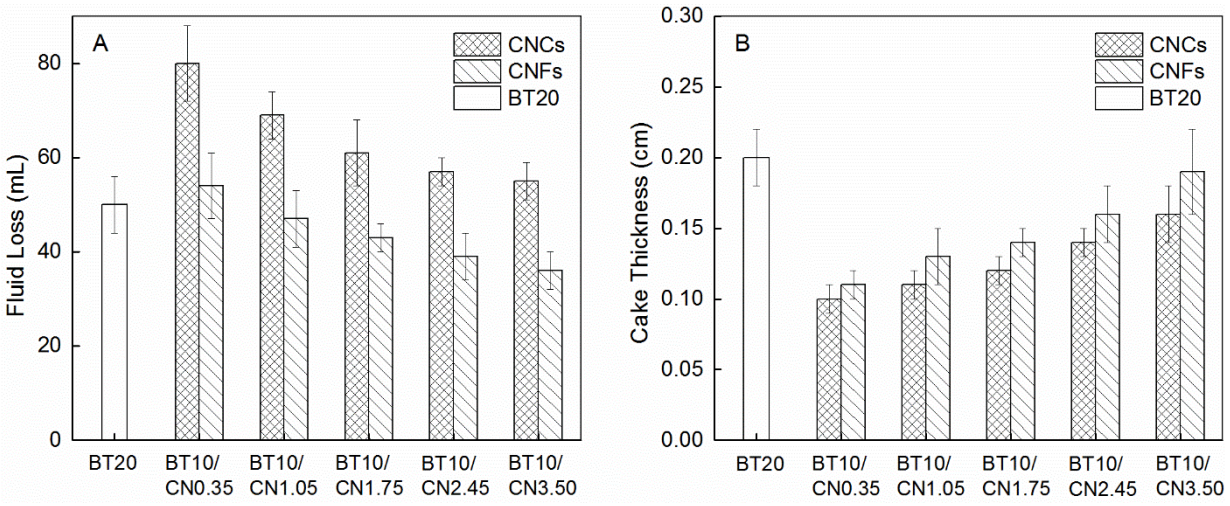

Figure 6 Fluid loss and cake thickness of the fluids under a higher temperature and pressure condition

The API fluid loss and cake thickness of the fluids at a higher temperature and pressure condition are shown in Figure 6. The control (BT20) had a filtrate volume of 50 mL at the end of 30 min testing time. When the BT content decreased by half, the filtrate spurted out quickly and continuously and the applied pressure could not go up to 6.9 MPa, making the measurement of fluid loss for BT10 unattainable. This indicated that 10 g of BT in the fluids was not enough to plug the pores (diameter 20 μm) of the ceramic disks in this study. However, this situation was avoided by adding CNPs into the fluids with 10 g of BT. The fluid loss decreased with increased concentrations of CNPs under a higher temperature and pressure condition. As the CNFs were above 1.05 g, the filtrate volume of the fluids was even lower than that of the control sample, with values ranging from 36-47 mL depending on loading levels of CNFs. In addition, the fluids with CNFs performed much better than those with CNCs, although the former had a little higher thickness of filter cakes than the later. The differences in filtrate volume between the fluids added with CNCs and CNFs at a higher temperature and pressure condition were related to their different pore plugging ability.

The penetration of the fluids into the porous ceramic disk is shown in Figure 7. It was seen that the solids mainly entered into the surface of the disks with a depth of 100-300 μm. Compared with the BT20

fluid, the fluids added with CNPs had a lower penetration depth, due to the reduced solid contents in the fluids. The fluids added with CNCs could not seal the pores in the disks completely because of their very small dimensions. On the contrary, the fluids with CNFs plugged the pores more efficiently with their long entangled nanofibers, contributing to the reduced fluid loss of the fluids with CNFs. Therefore, a decreased amount of BT from 20 g to 10 g with the addition of a very small fraction of CNFs (1.05-3.50 g) could reduce the fluid loss and formation damage with a less penetration depth. Additionally, it was worth mentioning that the effect of CNPs on pore plugging ability was dependent on the size of itself and pores of disks. Therefore, the size of CNPs could be tuned by changing the preparation conditions such as concentrations of sulfuric acid and time of acid hydrolysis to maximize the plugging capability for subsurface formations with different pore diameters.

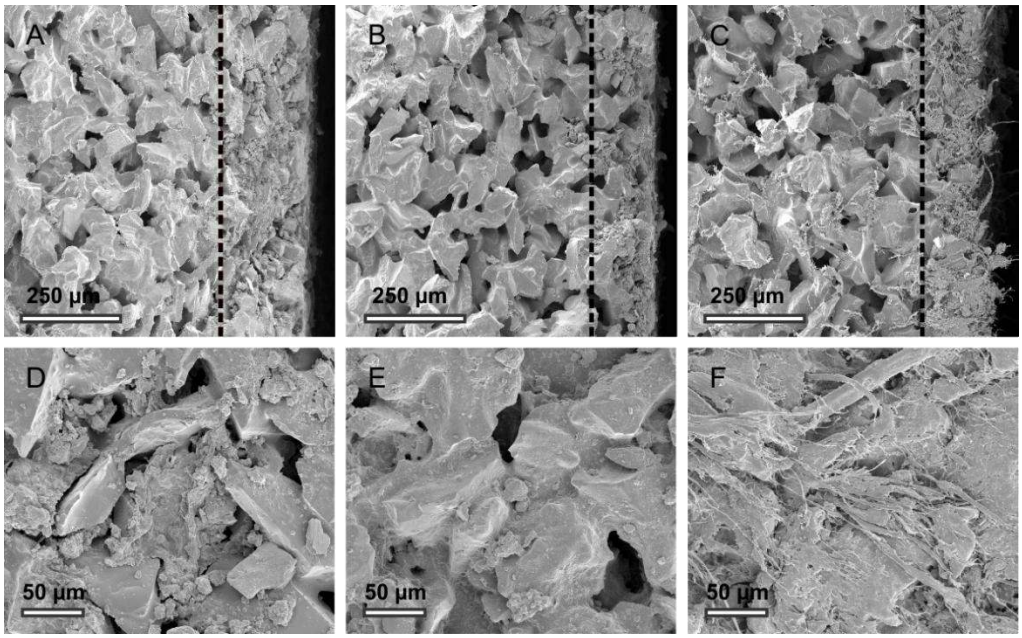

Figure 7 Cross sectional (A, B, and C) and surface (D, E, and F) FE-SEM images of the ceramic disks for BT20 (A and D), BT10/CNC3.50 (B and E), and BT10/CNF3.50 (C and F) at a higher temperature and pressure condition

4. Conclusions

Novel low cost, ecologically friendly, high performance water-based fluids were successfully fabricated by replacing half of BT in traditional fluids with low addition levels of CNPs. The CNPs played

an essential role in improving the rheological properties, reducing fluid loss, and minimizing formation damage of the drilling fluids. The fluids with CNPs showed similar non-Newtonian fluid behavior to the control fluid, due to the excellent shear thinning properties of water suspensions of CNPs. The viscosity, yield point, and gel strength of the fluids increased with an increasing concentration of CNPs. The fluids with CNCs has better flow properties due to their smaller dimensions and well dispersions than the fluids with CNFs having long and highly entangled nanofibers. As a result, the CNC added fluids exhibited lower values in viscosity, yield point, and initial gel strength for the former compared to the CNF added fluids. The high 10-min gel strength of the fluids with CNCs was attributed to the strong hydrogen bonding network formed in the fluids added with CNCs. For filtration properties, the fluid loss of the drilling fluids with CNPs was larger than that of the control fluid under LTLP conditions, due to the enhanced connectivity of pores in the filter cakes by the CNPs. However, the CNPs performed much better at a higher temperature and pressure condition, especially the CNFs. The long and highly intertwined CNFs plugged the pores in the ceramic disks more efficiently than CNCs, leading to lower fluid loss compared with the control fluid when the content of CNFs was above 1.05 g (per 350 ml water). Furthermore, the dimensions of CNPs could be controlled to maximize the plugging effect of subsurface formations with different pore sizes. Therefore, a novel pathway was provided to develop novel renewable biopolymer additives in water-based drilling fluids with enhanced performance and advantages of low cost and ecologically friendly.

Acknowledgment

This collaborative study was carried out with support from LSU Economic Development Assistantship program, Louisiana Board of Regents [LEQSF(2015-17)-RD-B-01], the USDA National Institute of Food and Agriculture McIntire Stennis project [1000017], and Key Biomass Energy Laboratory of Henan Province, Zhengzhou, China.

References

[1] A.T. Bourgoyne, K.K. Millheim, M.E. Chenevert, F.S. Young, Applied Drilling Engineering, first ed., Society of Petroleum Engineers, Richardson, 1991.

[2] J. González, F. Quintero, J. Arellano, R. Márquez, C. Sánchez, D. Pernía, Effects of interactions between solids and surfactants on the tribological properties of water-based drilling fluids, Colloids Surf. A 391 (2011) 216-223.

[3] M. Li, Q. Wu, K. Song, S.-Y. Lee, C. Jin, S. Ren, T. Lei, Soy protein isolate as fluid loss additive in bentonite-water based drilling fluids, ACS Appl. Mater. Interfaces 7 (2015) 24799–24809.

[4] J. Abdo, M.D. Haneef, Clay nanoparticles modified drilling fluids for drilling of deep hydrocarbon wells, Appl. Clay Sci. 86 (2013) 76-82.

[5] J. Abdo, R. Zaier, E. Hassan, H. AL-Sharji, A. Al-Shabibi, ZnO–clay nanocomposites for enhance drilling at HTHP conditions, Surf. Interface Anal. 46 (2014) 970-974.

[6] F. Sun, M. Lin, Z. Dong, J. Zhang, C. Wang, S. Wang, F. Song, Nanosilica-induced high mechanical strength of nanocomposite hydrogel for killing fluids, J. Colloid Interface Sci. 458 (2015) 45-52.

[7] M. Farbod, R. Kouhpeymani asl, A.R. Noghreh abadi, Morphology dependence of thermal and rheological properties of oil-based nanofluids of CuO nanostructures, Colloids Surf. A 474 (2015) 71-75.

[8] M. Li, Q. Wu, K. Song, C.F. De Hoop, S. Lee, Y. Qing, Y. Wu, Cellulose nanocrystals and polyanionic cellulose as additives in bentonite water-based drilling fluids: rheological modeling and filtration mechanisms, Ind. Eng. Chem. Res. 55 (2015) 133-143.

[9] E. Kasiralvalad, The great potential of nanomaterials in drilling & drilling fluid applications, Int. J. Nano Dimens. 5 (2014) 463-471.

[10] D.V. Kosynkin, G. Ceriotti, K.C. Wilson, J.R. Lomeda, J.T. Scorsone, A.D. Patel, J.E. Friedheim, J.M. Tour, Graphene oxide as a high-performance fluid-loss-control additive in water-based drilling fluids, ACS Appl. Mater. Interfaces 4 (2011) 222-227.

[11] B. Fazelabdolabadi, A.A. Khodadadi, M. Sedaghatzadeh, Thermal and rheological properties improvement of drilling fluids using functionalized carbon nanotubes, Appl. Nanosci. 5 (2015) 651-659.

374 [12] H. Mao, Z. Qiu, Z. Shen, W. Huang, H. Zhong, W. Dai, Novel hydrophobic associated polymer based
375 nano-silica composite with core-shell structure for intelligent drilling fluid under ultra-high temperature and
376 ultra-high pressure, Prog. Nat. Sci. Mater. Int. 25 (2015) 90-93.
377 [13] G. Cheraghian, M. Hemmati, M. Masihi, S. Bazgir, An experimental investigation of the enhanced oil
378 recovery and improved performance of drilling fluids using titanium dioxide and fumed silica nanoparticles,
379 J. Nanostruct. Chem. 3 (2013) 78.
380 [14] J.K.M. William, S. Ponmani, R. Samuel, R. Nagarajan, J.S. Sangwai, Effect of CuO and ZnO
381 nanofluids in xanthan gum on thermal, electrical and high pressure rheology of water-based drilling fluids,
382 J. Pet. Sci. Eng. 117 (2014) 15-27.
383 [15] S. Ponmani, R. Nagarajan, J.S. Sangwai, Effect of nanofluids of CuO and ZnO in polyethylene glycol
384 and polyvinylpyrrolidone on the thermal, electrical, and filtration-loss properties of water-based drilling
385 fluids, SPE J. (2015).
386 [16] R. Hartmann, J.A. Sirviö, R. Sliz, O. Laitinen, H. Liimatainen, A. Ämmälä, T. Fabritius, M. Illikainen,
387 Interactions between aminated cellulose nanocrystals and quartz: Adsorption and wettability studies,
388 Colloids Surf. A 489 (2016) 207-215.
389 [17] Z. Zhang, Q. Wu, K. Song, T. Lei, Y. Wu, Poly (vinylidene fluoride)/cellulose nanocrystals
390 composites: rheological, hydrophilicity, thermal and mechanical properties, Cellulose 22 (2015) 2431-2441.
391 [18] Z. Zhang, Q. Wu, K. Song, S. Ren, T. Lei, Q. Zhang, Using cellulose nanocrystals as a sustainable
392 additive to enhance hydrophilicity, mechanical and thermal properties of poly (vinylidene fluoride)/poly
393 (methyl methacrylate) blend, ACS Sustain. Chem. Eng. 3 (2015) 574-582.
394 [19] L. Wei, A.G. McDonald, A review on gafting of biofibers for biocomposites, Materials 9 (2016) 303.
395 [20] R.J. Moon, A. Martini, J. Nairn, J. Simonsen, J. Youngblood, Cellulose nanomaterials review:
396 structure, properties and nanocomposites, Chem. Soc. Rev. 40 (2011) 3941-3994.
397 [21] L. Wei, A.G. McDonald, N.M. Stark, Grafting of bacterial polyhydroxybutyrate (PHB) onto cellulose
398 via In situ reactive extrusion with dicumyl peroxide, Biomacromolecules 16 (2015) 1040-1049.

399 [22] L. Wei, N.M. Stark, A.G. McDonald, Interfacial improvements in biocomposites based on poly (3-
400 hydroxybutyrate) and poly (3-hydroxybutyrate-co-3-hydroxyvalerate) bioplastics reinforced and grafted
401 with α-cellulose fibers, Green Chem. 17 (2015) 4800-4814.
402 [23] M.T. Rincon-Torres, L.J. Hall, Cellulose nanowhiskers in well services, 2013, United States Patent US
403 20130196883 A1.
404 [24] L.J. Hall, Chitin nanocrystal containing wellbore fluids, 2014, United States Patent US 20140238677
405 A1.
406 [25] V. Lafitte, J.C. Lee, S.G. James, J.F. Del Valle, A.V. Yakovlev, M.K. Panga, G.H. Szabo, Fluids and
407 methods including nanocellulose, 2015, United States Patent US 20150072902 A1.
408 [26] M. Li, Q. Wu, K. Song, S. Lee, Y. Qing, Y. Wu, Cellulose nanoparticles: structure-morphology-
409 rheology relationships, ACS Sustain. Chem. Eng. 3 (2015) 821-832.
410 [27] Z. Zhang, K. Song, Y. Li, Q. Wu, Non-isothermal crystallization of poly (vinylidene fluoride)/poly
411 (methyl methacrylate)/cellulose nanocrystal nanocomposites, Int. J. Polym. Anal. Charact. 19 (2014) 332-
412 341.
413 [28] Y. Habibi, L.A. Lucia, O.J. Rojas, Cellulose nanocrystals: chemistry, self-assembly, and applications,
414 Chem. Rev. 110 (2010) 3479-3500.
415 [29] V. Mahto, V. Sharma, Rheological study of a water based oil well drilling fluid, J. Pet. Sci. Eng. 45
416 (2004) 123-128.
417 [30] S.B. Hamed, M. Belhadri, Rheological properties of biopolymers drilling fluids, J. Pet. Sci. Eng. 67
418 (2009) 84-90.
419 [31] M. Li, Q. Wu, K. Song, Y. Qing, Y. Wu, Cellulose nanoparticles as modifiers for rheology and fluid
420 loss in bentonite water-based fluids, ACS Appl. Mater. Interfaces 7 (2015) 5006-5016.
421 [32] M.M. Barry, Y. Jung, J.K. Lee, T.X. Phuoc, M.K. Chyu, Fluid filtration and rheological properties of
422 nanoparticle additive and intercalated clay hybrid bentonite drilling fluids, J. Pet. Sci. Eng. 127 (2015) 338-
423 346.